Tunneling anisotropic magnetoresistance of helimagnet tunnel junctions

Chenglong Jia and Jamal Berakdar
Institut für Physik, Martin-Luther Universität Halle-Wittenberg, Halle, 06120 Saale, Germany
(Received 2 November 2009; revised manuscript received 24 December 2009; published 17 February 2010)

We theoretically investigate the angular- and spin-dependent transport in normal-metal/helical-multiferroic/ferromagnetic heterojunctions. We find a tunneling anisotropic magnetoresistance (TAMR) effect due to the spiral magnetic order in the tunnel junction and to an effective spin-orbit coupling induced by the topology of the localized magnetic moments in the multiferroic spacer. The predicted TAMR effect is efficiently controllable by an external electric field due to the magnetoelectric coupling.

DOI: 10.1103/PhysRevB.81.052406 PACS number(s): 75.47.−m, 85.75.−d, 73.40.Gk

I. INTRODUCTION

Transport across two ferromagnetic layers separated by a tunnel barrier depends, in general, on the relative orientation of the layers magnetizations,[1] giving rise to the tunnel magnetoresistance (TMR) effect.[2] In the presence of spin-orbit interactions, TMR becomes spatially anisotropic.[3–5] Tunnel anisotropic magnetoresistance (TAMR) is observed not only in magnetic tunnel junctions with two ferromagnetic electrodes[3] but also in ferromagnetic/insulator/normal-metal systems such as Fe/GaAs/Au.[4] Here we show that TAMR is a distinctive feature of normal-metal/multiferroic/ferromagnetic heterojunctions with the particular advantage of being electrically controllable. The coexistence of coupled electric and magnetic order parameters in multiferroics[6] holds the promise of new opportunities for device fabrications.[7,8] Our interest is focused on helimagnetic multiferroic.[9,10] The topology of the local helical magnetic moments in these materials induces a resonant, momentum-dependent spin-orbit interaction.[8] The noncollinear magnetic order together with the induced spin-orbit coupling result in uniaxial TAMR with a C_{2v} symmetry. These two factors and their interplay determine the size and the sign of TAMR. In particular, a linear dependence on the spiral helicity results in an electrically[11] tunable spin-orbit interaction[8] by means of the magnetoelectric coupling, and thus TAMR is electrically controllable accordingly.

II. DEVICE PROPOSITION

The proposed multiferroic tunnel junction is sketched in Fig. 1. It consists of an ultrathin helical-multiferroic barrier sandwiched between a normal metallic (NM) layer and a ferromagnetic (FM) conductor. The ferroelectric polarization $\mathbf{P}$ in the multiferroic barrier creates, in general, surface charge densities $\pm|\mathbf{P}|$ which are screened by the induced charge at the two metal electrodes.[12] A depolarizing field emerges in the barrier. Taking the spontaneous electric polarization as $P_z=700\ \mu\mathrm{C/m}^2$ and the dielectric constant to be $\epsilon=30$ in the ferroelectric phase of $TbMnO_3$,[9] the potential drop generated by the depolarizing field in the multiferroic barrier is estimated to be on the energy scale of millielectron volt, which is much smaller than any other relevant energy scale in the system. In the present study, we neglect this potential modification and assume that the barrier potential has a rectangular shape with the height V_0. All energies are given with respect to the NM Fermi energy E_F. Based on this approximation, the Hamiltonians governing the carrier dynamics in the two electrodes and the oxide insulator have the following form:

$$H_{\mathrm{NM}} = -\frac{\hbar^2}{2m_e}\nabla^2, \quad \text{for } z<0,$$

$$H_{\mathrm{MF}} = -\frac{\hbar^2}{2m^*}\nabla^2 + J\mathbf{n_r}\cdot\boldsymbol{\sigma} + V_0, \quad \text{for } 0\le z\le d,$$

$$H_{\mathrm{FM}} = -\frac{\hbar^2}{2m_e}\nabla^2 - \Delta\mathbf{m}\cdot\boldsymbol{\sigma}, \quad \text{for } z>d, \tag{1}$$

where V_0 and d are the height and the width of the potential barrier [see Fig. 1(c)], and m_e is the free-electron mass. m^* is the effective electron mass of the oxide ($m^*/m_e\approx 10$) and $\boldsymbol{\sigma}$ is the vector of Pauli matrices. $\mathbf{m}=[\cos\phi,\sin\phi,0]$ is a unit vector defining the in-plane magnetization direction in the ferromagnet with respect to the [100] crystallographic direction. Δ is the half width of the Zeeman splitting in the ferromagnetic electrode. $J\mathbf{n_r}$ is the exchange field, where $\mathbf{n_r}$ is given by the multiferroic oxide local magnetization at each spiral layer (labeled by a integer number l) along the z axis,[11] i.e., $\mathbf{n_r}=(-1)^l[\sin\theta_r,0,\cos\theta_r]$ with $\theta_r=\bar{q}_m\cdot\mathbf{r}$ and $\bar{q}_m=[\bar{q},0,0]$ being the spiral spin-wave vector. The physical picture behind the term H_{MF} in Eq. (1) is that a tunneling electron experiences an exchange coupling at the sites of the localized noncollinear magnetic moments within the barrier. In effect this acts on the electron as a nonhomogenous magnetic field. Performing a local unitary transformation within the barrier,[8] one can also view the influence of the barrier as consisting of two terms a homogeneous Zeeman field, and a topology-induced spin-orbit coupling (SOC) that depends solely on the helical magnetic ordering. As shown in Ref. 8, this SOC depends linearly on the electron wave vector and on the helicity of the magnetic order[8] and is explicitly given by

$$\mathrm{SOC}\sim\frac{\hbar^2}{2m^*}\bar{q}k_x\sigma_y. \tag{2}$$

The dependence on k_x resembles the resonant semiconductor case when the Rashba[13] and Dresselhaus[14] spin-orbit interac-

 ©2010 The American Physical Society

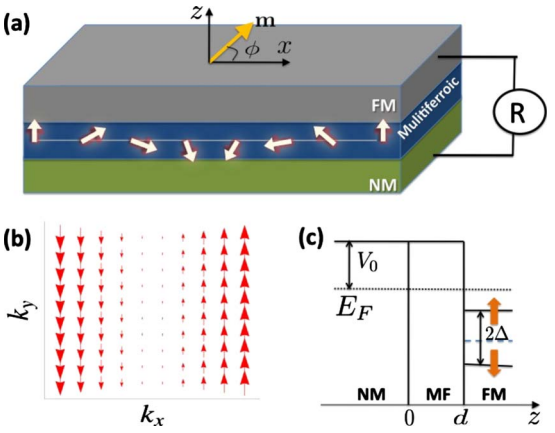

FIG. 1. (Color online) (a) Schematic of the helical-multiferroic tunnel junctions consisting of a normal metallic layer as the bottom electrode and a ferromagnetic layer for the top one. The vector **m** indicates the magnetization orientation specified by the angle ϕ in xy (FM) plane. The zx plane refers to the spiral plane of a multiferroic oxide. (b) The arrows show the induced resonant spin-orbit coupling, $qk_x\sigma_y$ in the multiferroic barrier. (c) The tunnel barrier potential profile.

tions have exactly equal strengths. Provided that the in-plane wave vector $\mathbf{k}_\parallel$ is nonzero, an electron in the oxide undergoes an exchange interaction with the local spiral magnetic moment and the induced spin-orbit coupling. So an electron spinor in the multiferroic barrier is determined by the following spin-dependence term,

$$H_{\mathrm{SO}}^{eff} = \mathbf{w}(\theta_r,\mathbf{k})\cdot\boldsymbol{\sigma}, \tag{3}$$

where

$$\mathbf{w}(\theta_r,\mathbf{k}) = [(-1)^l J\sin\theta_r, qk_x, (-1)^l J\cos\theta_r] \tag{4}$$

and $q=\frac{\hbar^2}{2m^*}\bar{q}$. With this effective spin-orbit interaction, we analyze the angular dependence of the electron tunneling through the helical-multiferroic barrier.

III. PHENOMENOLOGICAL THEORY

We assume the strength of the effective Zeeman field $|\mathbf{w}(\theta_r,\mathbf{k})|$ to be relatively smaller than the Fermi energy E_F and the band splitting Δ. Proceeding phenomenologically as in Ref. 5 one expands the transmissivity as a perturbative series of $\mathbf{m}\cdot\mathbf{w}(\theta_r,\mathbf{k})$. Up to the second order, the transmissivity reads

$$T(\mathbf{k},\mathbf{m}) = a_1^{(0)}(\mathbf{k}) + a_1^{(1)}(\mathbf{k})[\mathbf{m}\cdot\mathbf{w}(\theta_r,\mathbf{k})] + a_1^{(2)}(\mathbf{k})|\mathbf{w}(\theta_r,\mathbf{k})|^2 + a_2^{(2)}(\mathbf{k})|\mathbf{m}\cdot\mathbf{w}(\theta_r,\mathbf{k})|^2. \tag{5}$$

The expansion coefficients, $a_i^{(j)}$ $(i=1,2;\ j=0,1,2)$ satisfy the symmetry relations $a_i^{(j)}(k_x,k_y)=a_i^{(j)}(-k_x,-k_y)$, $a_i^{(j)}(k_x,k_y)=a_i^{(j)}(-k_x,k_y)$, and $a_i^{(j)}(k_x,k_y)=a_i^{(j)}(k_y,k_x)$. Based on the linear-response theory, the conductance $G(\phi)$ is found as

$$G(\phi) = \frac{e^2}{h}\int\frac{d^2\mathbf{k}_\parallel}{(2\pi)^2}\frac{d\theta_r}{2\pi}T(\mathbf{k},\mathbf{m}) = G_0 + G_{aniso}(\phi), \tag{6}$$

where G_0 is the angular-independent part of the conductance and

$$G_{aniso}(\phi) = g\ \mathrm{tr}[AM(\phi)] \tag{7}$$

is the anisotropic spin-orbit coupling contributions and $g=e^2/8\pi^3\hbar$. A and $M(\phi)$ are matrices whose elements are given, respectively, by

$$A_{ij} = \langle a_2^{(2)}(\mathbf{k})w_i w_j\rangle, \quad M_{ij}(\phi) = m_i m_j \ \ (i,j=x,y,z). \tag{8}$$

The notation $\langle\cdots\rangle$ stands for the integration over θ_r and $\mathbf{k}_\parallel$. Introducing $\mathbf{w}(\theta_r,\mathbf{k})$ and $\mathbf{m}$ into $G_{aniso}(\phi)$, Eq. (7), the anisotropic conductance can be rewritten as

$$G_{aniso}(\phi) = \alpha\cos^2\phi + \beta\sin^2\phi. \tag{9}$$

Considering the symmetry of the expansion coefficient $a_2^{(2)}(\mathbf{k})$, we obtain for the above expression, $\alpha = g\langle a_2^{(2)}(\mathbf{k})J^2\sin^2\theta_r\rangle$ and $\beta = g\langle a_2^{(2)}(\mathbf{k})q^2k_x^2\rangle$. Hence, the TAMR coefficient is given by

$$\mathrm{TAMR} = \frac{G(0)-G(\phi)}{G(\phi)} \approx \gamma(1-\cos 2\phi), \quad \gamma = \frac{\alpha-\beta}{2G_0}. \tag{10}$$

The above angular dependence of TAMR is quite general. The helical magnetic order and the induced spin-orbit interaction give rise to the anisotropy in the magentoconductance. However, as evident from Eq. (10), the TAMR coefficient γ depends on $(\alpha-\beta)$, i.e., contributions from the exchange interaction and the spin-orbit coupling term have opposite effects, which is confirmed by the following model calculations.

IV. ULTRATHIN BARRIERS

Experimental observations[7] indicate that thin-film multiferroics can retain both magnetic and ferroelectric properties down to a thickness of 2 nm (or even less). To get more insight in TAMR, we consider ultrathin tunneling barriers that can be approximated by a Dirac-delta function.[15] The effective spin-orbit interaction H_{MF}^{σ} throughout the multiferroic barrier reduces then to the plane of the barrier, $\tilde{H}_{\mathrm{MF}}^{\sigma} = \tilde{\mathbf{w}}(\theta_r,\mathbf{k})\cdot\boldsymbol{\sigma}\delta(z)$ with $\tilde{\mathbf{w}}(\theta_r,\mathbf{k}) = [\tilde{J}\sin\theta_r, \tilde{q}k_x, \tilde{J}\cos\theta_r]$. $\tilde{J}$ and $\tilde{q}$ are renormalized exchange and resonant spin-orbit coupling parameters, $\tilde{q}\approx\bar{q}V_0 d$ and $\tilde{J}\approx\langle J(z)\rangle_d$ referring to space and momentum averages with respect to the unperturbed states at the Fermi energy. In the following, we treat $\tilde{J}$ and $\tilde{q}$ as adjustable parameters. Obviously, the electron momentum parallel to the junction interfaces $\mathbf{k}_\parallel$ is conserved. Then the transverse electron wave functions in NM $(z<0)$ and FM $(z>0)$ regions can be written as

$$\Psi_{\mathrm{NM}}^{\sigma}(z) = e^{i\kappa z}\chi_\sigma + r_{\sigma,\sigma}e^{-i\kappa z}\chi_\sigma + r_{\sigma,\bar{\sigma}}e^{-i\kappa z}\chi_{\bar{\sigma}}, \tag{11}$$

$$\Psi_{\mathrm{FM}}^{\sigma}(z) = t_{\sigma,\sigma}e^{ik_{\sigma^z}z}\chi_\sigma + t_{\sigma,\bar{\sigma}}e^{ik_{\bar{\sigma}^z}z}\chi_{\bar{\sigma}} \tag{12}$$

with

$$\kappa = \sqrt{E/\frac{\hbar^2}{2m_e} - k_\parallel^2}, \tag{13}$$

$$k_\sigma = \sqrt{(E+\sigma\Delta)/\frac{\hbar^2}{2m_e} - k_\parallel^2} \tag{14}$$

and the spinors introduced as

$$\chi_\sigma = \frac{1}{\sqrt{2}}\begin{pmatrix} 1 \\ \sigma e^{i\phi} \end{pmatrix} \tag{15}$$

and correspond to an electron spin parallel ($\sigma=1$) or antiparallel ($\sigma=-1$) to the magnetization direction in the ferromagnetic electrode. The reflection ($r_{\sigma,\sigma}$ and $r_{\sigma,\bar{\sigma}}$) and transmission ($t_{\sigma,\sigma}$ and $t_{\sigma,\bar{\sigma}}$) coefficients can be analytically obtained from the continuity conditions for $\Psi(z)$ and $\Psi'(z)/m$ at $z=0$,[15]

$$\Psi^\sigma_{\mathrm{NM}}(0^-) = \Psi^\sigma_{\mathrm{FM}}(0^+), \tag{16}$$

$$\frac{\hbar^2}{2m_e}\frac{d\Psi^\sigma_{\mathrm{NM}}(z)}{dz}\bigg|_{z=0^-} + [V_0 d + \tilde{\mathbf{w}}(\theta_r,\mathbf{k})\cdot\boldsymbol{\sigma}]\Psi^\sigma_{\mathrm{NM}}(0^-) = \frac{\hbar^2}{2m_e}\frac{d\Psi^\sigma_{\mathrm{FM}}(z)}{dz}\bigg|_{z=0^+}. \tag{17}$$

The transmissivity of a spin-σ electron through the multiferric tunnel junctions reads

$$T_\sigma(E,\mathbf{k}_\parallel,\theta) = \Re\left[\frac{k_\sigma}{\kappa}|t_{\sigma,\sigma}|^2 + \frac{k_{\bar{\sigma}}}{\kappa}|t_{\sigma,\bar{\sigma}}|^2\right]. \tag{18}$$

For a small applied bias voltages, the conductance G is determined by the states at the Fermi energy E_F,[12,15,16]

$$G_\sigma = \frac{e^2}{h}\int \frac{d^2\mathbf{k}_\parallel}{(2\pi)^2}\frac{d\theta_r}{2\pi}T_\sigma(E_F,\mathbf{k}_\parallel,\theta_r). \tag{19}$$

Figure 2 (top) shows the TAMR angular dependence $\sim(1-\cos 2\phi)$, at $E_F=5.5$ eV, $\Delta=2$ eV, $V_0=0.5$ eV, and $d=2$ nm. It is clear that TAMR has C_{2v} symmetry. For small $\tilde{J}$, the spin-orbit interaction dominates the tunneling properties, we have positive TAMR. As $\tilde{J}$ increases, the size of TAMR is influenced by the interplay between the exchange field and the induced spin-orbit interaction. The TAMR is typically $\sim 0.1\%$, which is on the same order as in the Fe/GaAs/Au tunnel junctions that have been recently realized experimentally.[4,17] A transition from positive to negative TAMR is observed, which is consistent with the previous finding, i.e., Eq. (10) within the phenomenological model. On the other hand, the helicity of the spiral magnetic order $\tilde{q}$ in helimagnetic multiferroics is experimentally controllable by a small (~ 1 kV/cm) transverse electric field.[11] Consequently, we may electrically tune the spin-orbit coupling strength and thus TAMR in the helimagnet tunnel junctions [see Fig. 2 (bottom)].

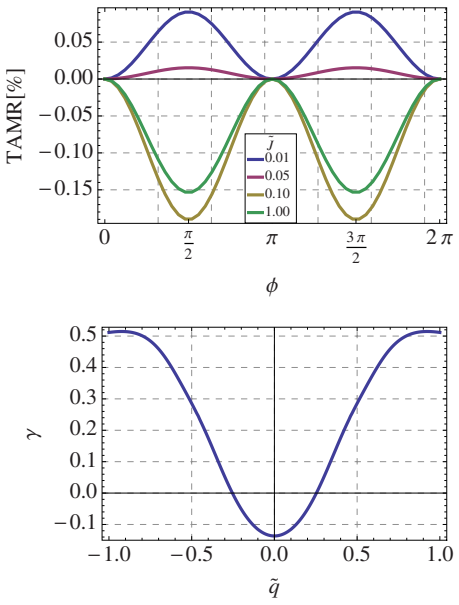

FIG. 2. (Color online) The angular dependence of TAMR on different strengths of the exchange field $\tilde{J}$(eV) and on the coefficient γ that enters the TAMR due to the competition between the exchange field and the induced spin-orbit interaction. The used numerical values are $E_F=5.5$ eV, $\Delta=2$ eV, $V_0=0.5$ eV, and $d=2$ nm. Top: $\tilde{q}=0.28$. Bottom: $\tilde{J}=0.1$ eV.

V. CONCLUSIONS

We studied the electron-tunneling properties through helical-multiferroic junctions. The spiral magnetic ordering and the induced spin-orbit interaction in the multiferroic barrier lead to the TAMR effect. Due to the magnetoelectric coupling, the strength of the induced spin-orbit coupling is electrically controllable which renders a tunable TAMR by an external electric field.

ACKNOWLEDGMENT

This research is supported by the DFG (Germany) under SFB 762.

[1] M. Julliere, Phys. Lett. A **54**, 225 (1975).
[2] I. Žutić, J. Fabian, and S. Das Sarma, Rev. Mod. Phys. **76**, 323 (2004); S. Parkin, MRS Bull. **31**, 389 (2006).
[3] L. Brey, C. Tejedor, and J. Fernández-Rossier, Appl. Phys. Lett. **85**, 1996 (2004); C. Gould, C. Rüster, T. Jungwirth, E. Girgis, G. M. Schott, R. Giraud, K. Brunner, G. Schmidt, and L. W. Molenkamp, Phys. Rev. Lett. **93**, 117203 (2004); C. Rüster, C. Gould, T. Jungwirth, J. Sinova, G. M. Schott, R. Giraud, K. Brunner, G. Schmidt, and L. W. Molenkamp, *ibid.* **94**, 027203 (2005); H. Saito, S. Yuasa, and K. Ando, *ibid.* **95**,

086604 (2005).
[4] J. Moser, A. Matos-Abiague, D. Schuh, W. Wegscheider, J. Fabian, and D. Weiss, Phys. Rev. Lett. **99**, 056601 (2007); M. Wimmer, M. Lobenhofer, J. Moser, A. Matos-Abiague, D. Schuh, W. Wegscheider, J. Fabian, K. Richter, and D. Wiss, Phys. Rev. B **80**, 121301(R) (2009).
[5] A. Matos-Abiague, M. Gmitra, and J. Fabian, Phys. Rev. B **80**, 045312 (2009).
[6] Y. Tokura, Science **312**, 1481 (2006); W. Eerenstein, N. D. Mathur, and J. F. Scott, Nature (London) **442**, 759 (2006); S.-W. Cheong and M. Nostovoy, Nature Mater. **6**, 13 (2007).
[7] H. Béa, M. Bibes, M. Sirena, G. Herranz, K. Bouzehouane, E. Jacquet, S. Fusil, P. Paruch, M. Dawber, J.-P. Contour, and A. Barthélémy, Appl. Phys. Lett. **88**, 062502 (2006); F. Yang, M. H. Tang, Z. Ye, Y. C. Zhou, X. J. Zhang, J. X. Tang, J. J. Zhang, and J. He, J. Appl. Phys. **102**, 044504 (2007); M. Gajek, M. Bibes, S. Fusil, K. Bouzehouane, J. Fontcuberta, A. Barthélémy, and A. Fert, Nature Mater. **6**, 296 (2007).
[8] C. Jia and J. Berakdar, Appl. Phys. Lett. **95**, 012105 (2009); Phys. Rev. B **80**, 014432 (2009).
[9] T. Kimura, T. Goto, H. Shintani, K. Ishizaka, T. Arima, and Y. Tokura, Nature (London) **426**, 55 (2003).
[10] T. Goto, T. Kimura, G. Lawes, A. P. Ramirez, and Y. Tokura, Phys. Rev. Lett. **92**, 257201 (2004); M. Kenzelmann, A. B. Harris, S. Jonas, C. Broholm, J. Schefer, S. B. Kim, C. L. Zhang, S.-W. Cheong, O. P. Vajk, and J. W. Lynn, *ibid.* **95**, 087206 (2005); Y. Yamasaki, S. Miyasaka, Y. Kaneko, J.-P. He, T. Arima, and Y. Tokura, *ibid.* **96**, 207204 (2006); J. Hemberger, F. Schrettle, A. Pimenov, P. Lunkenheimer, V. Yu. Ivanov, A. A. Mukhin, A. M. Balbashov, and A. Loidl, Phys. Rev. B **75**, 035118 (2007).
[11] Y. Yamasaki, H. Sagayama, T. Goto, M. Matsuura, K. Hirota, T. Arima, and Y. Tokura, Phys. Rev. Lett. **98**, 147204 (2007); S. Seki, Y. Yamasaki, M. Soda, M. Matsuura, K. Hirota, and Y. Tokura, *ibid.* **100**, 127201 (2008); H. Murakawa, Y. Onose, and Y. Tokura, *ibid.* **103**, 147201 (2009).
[12] M. Ye. Zhuravlev, R. F. Sabirianov, S. S. Jaswal, and E. Y. Tsymbal, Phys. Rev. Lett. **94**, 246802 (2005); H. Kohlstedt, N. A. Pertsev, J. Rodríguez Contreras, and R. Waser, Phys. Rev. B **72**, 125341 (2005).
[13] Y. A. Bychkov and E. I. Rashba, J. Phys. C **17**, 6039 (1984).
[14] G. Dresselhaus, Phys. Rev. **100**, 580 (1955).
[15] A. Matos-Abiague and J. Fabian, Phys. Rev. B **79**, 155303 (2009).
[16] C. B. Duke, *Tunneling in Solids* (Academic, New York, 1996).
[17] V. Laukhin, V. Skumryev, X. Martí, D. Hrabovsky, F. Sánchez, M. V. García-Cuenca, C. Ferrater, M. Varela, U. Lüders, J. F. Bobo, and J. Fontcuberta, Phys. Rev. Lett. **97**, 227201 (2006).